Residence time estimates for asymmetric simple exclusion dynamics on stripes

Document status and date:
Published: 01/01/2014

Document Version:
Publisher's PDF, also known as Version of Record (includes final page, issue and volume numbers)

Please check the document version of this publication:

• A submitted manuscript is the version of the article upon submission and before peer-review. There can be important differences between the submitted version and the official published version of record. People interested in the research are advised to contact the author for the final version of the publication, or visit the DOI to the publisher's website.
• The final author version and the galley proof are versions of the publication after peer review.
• The final published version features the final layout of the paper including the volume, issue and page numbers.

[Link to publication](#)

EINDHOVEN UNIVERSITY OF TECHNOLOGY
Department of Mathematics and Computer Science

Residence time estimates for asymmetric simple exclusion dynamics on stripes

by

E.N.M. Cirillo, A. Muntean, R.A. van Santen, A. Sengar

Residence time estimates for asymmetric simple exclusion dynamics on stripes

Emilio N.M. Cirillo

Dipartimento di Scienze di Base e Applicate per l'Ingegneria, Sapienza Università di Roma, via A. Scarpa 16, I–00161, Roma, Italy.
E mail: emilio.cirillo@uniroma1.it

Adrian Muntean

Department of Mathematics and Computer Science, (CASA) Centre for Analysis, Scientific computing and Applications, Institute for Complex Molecular Systems Eindhoven University of Technology, P.O. Box 513, 5600 MB Eindhoven, The Netherlands
E mail: a.muntean@tue.nl

Rutger van Santen

Institute of Complex Molecular Systems and Faculty of Chemical Engineering, Eindhoven University of Technology, P.O. Box 513, 5600 MB Eindhoven, The Netherlands
E mail: R.A.v.Santen@tue.nl

Aditya Sengar

Indian Institute of Technology Delhi, India
E mail: adityasengariitd@gmail.com

Abstract. The target of our study is to approximate numerically and, in some particular physically relevant cases, also analytically, the residence time of particles undergoing an asymmetric simple exclusion dynamics on a stripe. The source of asymmetry is twofold: (i) the choice of boundary conditions (different reservoir levels) and (ii) the strong anisotropy from a nonlinear drift with prescribed directionality. We focus on the effect of the choice of anisotropy in the flux on the asymptotic behavior of the residence time with respect to the length of the stripe. The topic is relevant for situations occurring in pedestrian flows or biological transport in crowded environments, where lateral displacements of the particles occur predominantly affecting therefore in an essentially way the efficiency of the overall transport mechanism.

Keywords: residence time, simple exclusion random walks, deposition model, complexity, self–organization

1. Introduction

The efficiency of transport of active matter in microscopic systems is an issue of paramount importance in a number of fields of science including biology, chemistry, and logistics. Looking particularly at drug–delivery design scenarios [19], ion moving in molecular cytosol [1–3], percolation of aggressive acids through reactive porous media [14], the traffic of pedestrians in regions with drastically reduced visibility (e.g., in the dark or in the smoke) [9, 10, 20] (see also the problem of traffic of cars on single–lane highways [23]), we see that the efficiency of a medical treatment, the properties of ionic currents thorough cellular membranes, the durability of a highly permeable material, or the success of the evacuation of a crowd of humans, strongly depends on the time spent by the individual particle (colloid, ion, acid molecule, or human being) in the constraining geometry (body, molecule, fabric, or corridor).

In this framework, we focus our attention on the study of the simplest two–dimensional scenario that mimics alike dynamics. The *Gedankenexperiment* we make is the following: we imagine a vertical stripe whose top and bottom entrances are in touch with infinite particle reservoirs at constant densities. Assume particles are driven downwards by the boundary densities difference and/or an external constant and uniform field (electrical, gravitational, generally–accepted crowd opinion, ...). Let the *residence time* be the typical time a particle entering the stripe at stationarity from the top boundary needs to exit through the bottom one. In this framework, under the assumption that particles in the stripe interact only via hard–core exclusion, we study the *ballistic–like* versus the *diffusion–like* dependence of the residence time on the external driving force (main source of anisotropy in the system), on the length of the stripe, on the horizontal diffusion, and, finally, on the choice of the boundary condition at the bottom.

We recover the structure of the fluxes as well as the residence times proven mathematically by Derrida and co–authors in [11] for the asymmetric simple exclusion model on the line; see also [17] for a more recent approach. In chemistry single file diffusion has been demonstrated for zeolite catalysts [18] to dramatically reduce the rate of a reaction. This happens in particular when zeolitic microporous systems are used with linear micropores with dimensions that are similar as the size of the molecules that are converted. Since they cannot pass single file inhibition occurs (see, for instance, [16]).

Additionally, we discover new effects that are purely due to the choice of the two–dimensional geometry and which are therefore absent in a 1D lattice. The most prominent is the non–monotonic behavior in changes in the horizontal displacement probability in the

bouncing back regime reported in Section 6.3. This effect is seen when particles accumulate next to the bottom exit of the stripe: in this situation crowding produces a sort of bouncing back effect to particles trying to exit the stripe. We observe that, in such a case, increasing the frequency of horizontal movements help particles to overcome obstacles and to find their way to the exit.

To investigate this model, we employ several working techniques including Taylor series truncations for the derivation of the mean–field equations, ODE analysis of the stationary case, estimates involving the structure of the stationary measure for birth and death processes on a line, as well as Monte Carlo simulations to exploit the resources offered by the various parameter regimes. In dimension one, this model has been widely studied both by the mathematical and physical communities, see e.g. [7, 11, 12, 17]. In two space dimensions, the situation is very much unexplored especially in the asymmetric case. We deal with this precise problem and we give a rather complete description of the phenomenon. Our results, which are based on a thorough study of a simplified model and extensive Monte Carlo simulations, open new mathematical problems concerning the typical time a particle need to cross a region in hard–core repulsion regime.

The paper is structured in the following fashion: we describe the dynamics of our stochastic lattice model in Section 2. Section 3 is concerned primarily with the derivation of the mean field equations governing the macroscopic evolution of the density. This is also the place where we study the stationary mean field behavior, the thermalization time of the system as well as the numerical testing of the accuracy of the mean field prediction of the stationary density profile. In Section 4 we make the direct analogy between our scenario and a biased birth and death model for which we can calculate explicitly the unique invariant measure and the use this object to obtain analytical lower and upper bounds on the residence time for three distinct physically relevant scenarios, viz. (i) a homogeneous case, (ii) a linear case, (iii) a totally asymmetric case. The core of the paper is Section 5 and Section 6. Herein we use inspiration from the handling of the biased birth and death model to get approximate analytical bounds on the residence time for our problem for selected parameter regimes. Finally, we explore numerically the residence time for all parameter regimes and compare the rests with the derived analytical bounds. Two Appendices containing additional numerical estimates of residual times close the paper.

2. The model

Let L_1, L_2 be two positive integers. Let $\Lambda \subset \mathbb{Z}^2$ denote the *stripe* $\{1, \ldots, L_1\} \times \{1, \ldots, L_2\}$. We say that the coordinate directions 1 and 2 of the stripe are respectively the *horizontal* and the *vertical* direction. We shall accordingly use the words *top*, *bottom*, *left*, and *right*.

On Λ we define a discrete time stochastic process controlled by the parameters

$$\varrho_{\mathrm{u}}, \varrho_{\mathrm{d}} \in [0,1] \quad \text{and} \quad h, u, d \in [0,1] \quad \text{such that } h + u + d = 1$$

whose meaning will be explained below.

The *configuration* of the system at time $t \in \mathbb{Z}_+$ is given by the positive integer $n(t)$ denoting the number of particles in the system at time t and by the two collections of integers $x_1(1,t),\dots,x_1(n(t),t) \in \{1,\dots,L_1\}$ and $x_2(1,t),\dots,x_2(n(t),t) \in \{1,\dots,L_2\}$ denoting, respectively, the horizontal and the vertical coordinates of the $n(t)$ particles in the stripe Λ at time t. The i–th particle, with $i = 1,\dots,n(t)$, is then associated with the site $(x_1(i,t), x_2(i,t)) \in \Lambda$ which is called *position* of the particle at time t. A site associated with a particle a time t will be said to be *occupied* at time t, otherwise we shall say that it is *free* or *empty* at time t. We let $n(0) = 0$.

At each time $t \geq 1$ we first set $n(t) = n(t-1)$ and then repeat the following algorithm $n(t-1)$ times. One of the three actions *insert a particle through the top boundary*, *insert a particle through the bottom boundary*, and *move a particle in the bulk* is performed with the corresponding probabilities $\varrho_{\mathrm{u}} L_1 / (\varrho_{\mathrm{u}} L_1 + \varrho_{\mathrm{d}} L_1 + n(t))$, $\varrho_{\mathrm{d}} L_1 / (\varrho_{\mathrm{u}} L_1 + \varrho_{\mathrm{d}} L_1 + n(t))$, and $n(t) / (\varrho_{\mathrm{u}} L_1 + \varrho_{\mathrm{d}} L_1 + n(t))$.

Insert a particle through the top boundary. Chose at random with uniform probability the integer $i \in \{1,\dots,L_1\}$ and, if the site $(1,i)$ is empty, with probability d set $n(t) = n(t) + 1$ and add a particle to site $(1,i)$.

Insert a particle through the bottom boundary. Chose at random with uniform probability the integer $i \in \{1,\dots,L_1\}$ and, if the site (L_2,i) is empty, with probability u set $n(t) = n(t) + 1$ and add a particle to site (L_2,i).

Move a particle in the bulk. Chose at random with uniform probability one of the $n(t)$ particles in the bulk. The chosen particle is moved according to the following rule: one of the four neighboring sites of the one occupied by the particle is chosen at random with probability $h/2$ (left), u (up), $h/2$ (right), and d (down). If the chosen site is in the stripe (not on the boundary) and it is free, the particle is moved there leaving empty the site occupied at time t. If the chosen site is on the boundary of the stripe the dynamics is defined as follows: the left boundary $\{(0,z_2),\ z_2 = 1,\dots,L_2\}$ and the right boundary $\{(L_1+1,z_2),\ z_2 = 1,\dots,L_2\}$ are *reflecting* (homogeneous Neumann boundary conditions) in the sense that a particle trying to jump there is not moved. The bottom and the top boundary conditions are stochastic in the sense that when a particle tries to jump to a site $(z_1,0)$, with $z_1 = 1,\dots,L_1$, such a site has to be considered occupied with probability ϱ_{u} and free with probability $1 - \varrho_{\mathrm{u}}$, whereas when a particle tries to jump to a site (z_1, L_2+1), with $z_1 = 1,\dots,L_1$, such a site has to be considered occupied with probability ϱ_{d} and free with probability $1 - \varrho_{\mathrm{d}}$. If the arrival site

is considered free the particle trying to jump there is removed by the stripe Λ (it is said to *exit* the system) and the number of particles is reduced by one, namely, $n(t) = n(t) - 1$. If the arrival site is occupied the particle is not moved.

We gave the definition of the model in an algorithmic way, but note that the model is a Markov chain $\omega_0, \omega_1, \ldots, \omega_t, \ldots$ on the *state* or *configuration space* $\Omega := \{0, 1\}^\Lambda$ with transition probability that can be deduced by the algorithmic definition.

3. Mean Field estimates

Let the *occupation number* of the site $(z_1, z_2) \in \Lambda$ at time t be equal to 1 if such a site is occupied by a particle at time t and to 0 otherwise. Let, also, $m_t(z_1, z_2)$ be the expectation of the occupation number at site $(z_1, z_2) \in \Lambda$ at time $t \geq 0$. This quantity is obviously well defined if one thinks to the model as a stochastic process. But if one wants a more intuitive idea of what such a quantity is, one can think of running the dynamics many times independently and then computing equal time averages with respect to these different realizations of the process. The mean over those independent realizations of the occupation number at site (z_1, z_2) at time t will be $m_t(z_1, z_2)$.

Now, we set up a Mean Field computation for such a mean occupation time m_t. We shall follow [22], but it is worth noting that, in dimension one and on the infinite volume $\mathbb{Z}$, the equation we shall obtain is proven rigorously to be the hydrodynamic limit of the discrete space random process [21] (see, also, [6, Section 2.4]).

We need to reproduce and slightly generalize the approach in [22] since there a particular choice for the horizontal probability has been considered, whereas we need a more general result. Let the *drift* be

$$\delta = \frac{d - u}{d + u} \quad . \tag{3.1}$$

This is indeed the physically meaningful definition of drift, since it is the ratio between the difference of the probabilities to move down and up and the total probability to perform a vertical displacement. Note that, since $d + u = 1 - h$, a simple computation yields

$$d = \frac{1 - h}{2}(1 + \delta) \quad \text{and} \quad u = \frac{1 - h}{2}(1 - \delta) \quad . \tag{3.2}$$

Let p the probability that at time t a specific particle is updated: in our dynamics such a probability is of order one, since at each time we update at random $n(t - 1)$ particles, where, we recall, $n(t)$ is the number of particles in the system at time t. The Mean Field approximation consists in writing, for an arbitrary point (z_1, z_2) in the bulk of Λ, the following

balance equation:

$$
\begin{aligned}
m_{t+1}&(z_1, z_2) - m_t(z_1, z_2) \\
&= p(h/2)m_t(z_1 - 1, z_2)[1 - m_t(z_1, z_2)] + pdm_t(z_1, z_2 - 1)[1 - m_t(z_1, z_2)] \\
&\quad + p(h/2)m_t(z_1 + 1, z_2)[1 - m_t(z_1, z_2)] + pum_t(z_1, z_2 + 1)[1 - m_t(z_1, z_2)] \\
&\quad - p(h/2)m_t(z_1, z_2)[1 - m_t(z_1 + 1, z_2)] - pdm_t(z_1, z_2)[1 - m_t(z_1, z_2 + 1)] \\
&\quad - p(h/2)m_t(z_1, z_2)[1 - m_t(z_1 - 1, z_2)] - pum_t(z_1, z_2)[1 - m_t(z_1, z_2 - 1)] \\
&= p(h/2)[m_t(z_1 + 1, z_2) - 2m_t(z_1, z_2) + m_t(z_1 - 1, z_2)] \\
&\quad + p((1 - h)/2)[m_t(z_1, z_2 + 1) - 2m_t(z_1, z_2) + m_t(z_1, z_2 - 1)] \\
&\quad - p\delta((1 - h)/2)\{[1 - m_t(z_1, z_2)][m_t(z_1, z_2 + 1) - m_t(z_1, z_2 - 1)] \\
&\qquad + m_t(z_1, z_2)[(1 - m_t(z_1, z_2 + 1)) - (1 - m_t(z_1, z_2 - 1))]\} \ .
\end{aligned}
$$

Now, we multiply and divide suitably the space and time units Δ and τ to obtain

$$
\begin{aligned}
[m_{t+1}&(z_1, z_2) - m_t(z_1, z_2)]/\tau \\
&= [ph\Delta^2/(2\tau)]\,[m_t(z_1 + 1, z_2) - 2m_t(z_1, z_2) + m_t(z_1 - 1, z_2)]/\Delta^2 \\
&\quad + [p(1 - h)\Delta^2/(2\tau)]\,[m_t(z_1, z_2 + 1) - 2m_t(z_1, z_2) + m_t(z_1, z_2 - 1)]/\Delta^2 \\
&\quad - [2p\delta(1 - h)\Delta/(2\tau)]\,\{[1 - m_t(z_1, z_2)][m_t(z_1, z_2 + 1) - m_t(z_1, z_2 - 1)] \\
&\qquad + m_t(z_1, z_2)[(1 - m_t(z_1, z_2 + 1)) - (1 - m_t(z_1, z_2 - 1))]\}/(2\Delta) \ .
\end{aligned}
$$

Finally, if we assume that the scales Δ and τ and the drift δ tend to zero, with respect to some scale parameter, so that

$$
p\Delta^2/(2\tau) \to 1 \quad \text{and} \quad \delta/\Delta \to \bar{\delta} \ ,
$$

we find the Mean Field limiting equation

$$
\frac{\partial m}{\partial t} = h\frac{\partial^2 m}{\partial z_1^2} + (1 - h)\frac{\partial^2 m}{\partial z_2^2} - 2\bar{\delta}(1 - h)\frac{\partial}{\partial z_2}[m(1 - m)] \ . \tag{3.3}
$$

It is worth noting that the above equation is a diffusion–like equation with an anisotropic and nonlinear flux. From the physical point of view the most interesting remark is that the diffusion part of the equation is linear. The effect of the drift is captured in nonlinear transport term. This term vanishes when $\delta = 0$, so that linearity is approximatively restored at very small δ.

Considering that the space scale Δ is indeed the length unit in our discrete model, we compare the numerical results with the solutions of the above limiting equation with $\bar{\delta} = \delta$, namely,

$$
\frac{\partial m}{\partial t} = h\frac{\partial^2 m}{\partial z_1^2} + (1 - h)\frac{\partial^2 m}{\partial z_2^2} - 2\delta(1 - h)\frac{\partial}{\partial z_2}[m(1 - m)] \ . \tag{3.4}
$$

Since in the top and bottom boundary densities are constant in space (along the border), the stationary solutions to (3.4) do not depend on the space variable z_1. We call $\varrho(z_2)$ a *density profile* of the stationary Mean Field equation

$$\varrho'' - b\frac{\mathrm{d}}{\mathrm{d}z_2}\varrho(1-\varrho) = 0 \quad \text{with} \quad b = \frac{2\delta(1-h)}{1-h} = 2\delta \tag{3.5}$$

with the Dirichlet boundary conditions

$$\varrho(0) = \varrho_{\mathrm{u}} \quad \text{and} \quad \varrho(L_2+1) = \varrho_{\mathrm{d}} \ . \tag{3.6}$$

3.1. Stationary Mean Field behavior

Finding the stationary profile $\varrho(z_2)$ means solving the ordinary differential equation (3.5) with the Dirichlet boundary conditions (3.6). We integrate equation (3.5) once with respect to the space variable from 0 to z_2 to get

$$\varrho' = b\varrho(1-\varrho) + c \quad \text{where} \quad c = \varrho'(0) - b\varrho_{\mathrm{u}}(1-\varrho_{\mathrm{u}}) \ . \tag{3.7}$$

The structure of the solutions of this equation, namely the phase space trajectories, can be studied via a simple qualitative analysis (see, for instance, [4, Chapter 1]). Let $f(\varrho) = b\varrho(1-\varrho) + c$ be the right hand side of (3.7). Five different situations have to be considered: $c > 0$, $c = 0$, $c < 0$ and $b/4+c > 0$, $b/4+c = 0$, and $b/4+c < 0$. In Figure 3.1 the phase diagram in the extended phase space is shown in the two cases $c < 0$ and $b/4 + c > 0$, $b/4 + c < 0$.
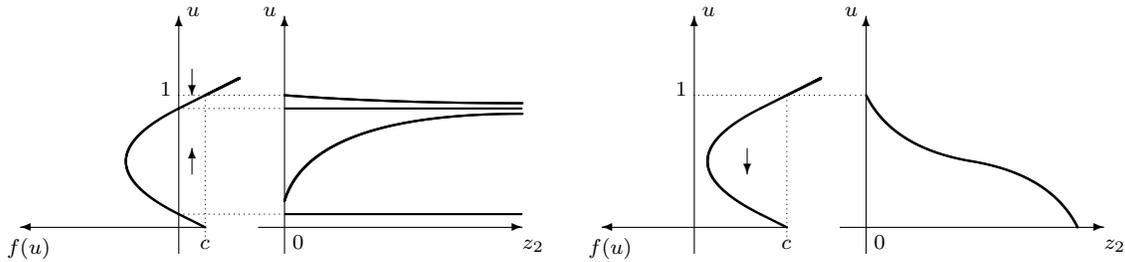
Figure 3.1: Phase diagram corresponding to (3.5). The case $c < 0$ and $b/4 + c > 0$ is depicted on the left. The case $b/4 + c < 0$ is depicted on the right.

Now, we find the solution of the stationary equation in the cases of interest. From the picture it is clear that:

- if $1 \geq \varrho_{\mathrm{u}} > 1/2 > \varrho_{\mathrm{d}} \geq 0$ the constant c has to be such that $b/4 + c < 0$;

- if $1 \geq \varrho_{\mathrm{u}} > \varrho_{\mathrm{d}} > 1/2$ the constant c has to be such that either $b/4 + c < 0$ or $0 > c > -b/4$.

It is important to remark that in the first case the constant c has to be necessarily larger that $-b/4$, while in the second case there are two different possibilities, so that we will have to decide which is the correct one.

Case $1 \geq \varrho_u > 1/2 > \varrho_d \geq 0$. Assume $b/4 + c < 0$, by performing a standard computation we find the solution

$$\arctan \frac{\varrho(z_2) - 1/2}{\sqrt{-c/b - 1/4}} = \arctan \frac{\varrho_u - 1/2}{\sqrt{-c/b - 1/4}} - b\sqrt{-\frac{c}{b} - \frac{1}{4}} z_2 \tag{3.8}$$

with the constant c given by

$$\arctan \frac{\varrho_u - 1/2}{\sqrt{-c/b - 1/4}} - \arctan \frac{\varrho_d - 1/2}{\sqrt{-c/b - 1/4}} = b\sqrt{-\frac{c}{b} - \frac{1}{4}}(L_2 + 1) \ . \tag{3.9}$$

It is not difficult to verify the following facts: as a function of $c \in [-\infty, -b/4]$ the left hand side of (3.9) is a monotone function increasing from 0 to $-\pi$. Hence, (3.9) admits a unique solution in this case.

We can then conclude that in such a case the stationary Mean Field equation has the unique solution given by (3.8) with the constant c as in (3.9).

Case $1 \geq \varrho_u > \varrho_d > 1/2$. In this case, the left hand side of (3.9) tends to zero for $c \to -b/4$, so that (3.9) has a solution provided

$$\lim_{c \to -b/4} \frac{\arctan \dfrac{\varrho_u - 1/2}{\sqrt{-c/b - 1/4}} - \arctan \dfrac{\varrho_d - 1/2}{\sqrt{-c/b - 1/4}}}{b\sqrt{-\dfrac{c}{b} - \dfrac{1}{4}}(L_2 + 1)} > 1 \ .$$

By computing the limit above, we get the condition

$$\frac{\varrho_u - \varrho_d}{b(L_2 + 1)(\varrho_u - 1/2)(\varrho_d - 1/2)} > 1 \ . \tag{3.10}$$

We recall, now, that in this case it is also possible to find a solution of the Mean Field equation (3.5) with $0 > c > -b/4$. By a standard computation we find the solution

$$\varrho(x) = \frac{u_2 - u_1 \exp\{-bz_2(u_2 - u_1) - \log[(\varrho_u - u_1)/(\varrho_u - u_2)]\}}{1 - \exp\{-bz_2(u_2 - u_1) - \log[(\varrho_u - u_1)/(\varrho_u - u_2)]\}} \ , \tag{3.11}$$

where

$$u_1 = \frac{1 - \sqrt{1 + 4c/b}}{2} < u_2 = \frac{1 + \sqrt{1 + 4c/b}}{2} \ , \tag{3.12}$$

where the constant c, hidden in the expressions of u_1 and u_2, can be obtained by requiring $u(L_2 + 1) = \varrho_d$, namely,

$$\varrho_d = \frac{u_2 - u_1 \exp\{-b(L_2 + 1)(u_2 - u_1) - \log[(\varrho_u - u_1)/(\varrho_u - u_2)]\}}{1 - \exp\{-b(L_2 + 1)(u_2 - u_1) - \log[(\varrho_u - u_1)/(\varrho_u - u_2)]\}} \ . \tag{3.13}$$
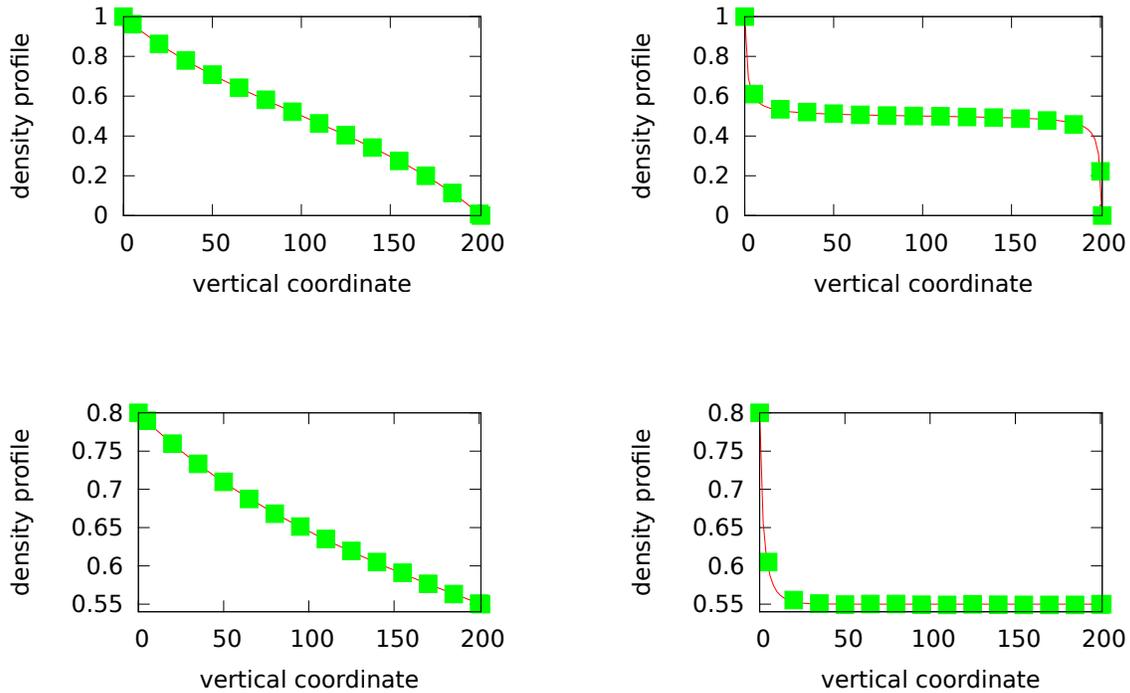
Figure 3.2: Density profiles. Comparison with numerical results (dots) and the Mean Field solution (solid lines). The cases described in Section 3.2 are considered: (i) top left, (ii) top right, (iii) bottom left, and (iv) bottom right.

By computing the limit, for $c \to -b/4$ of the ratio on the right hand side of (3.13), it is possible to show that such a limit is either larger or smaller than ϱ_d if and only if the equality (3.10) is satisfied. This occurrence is related to the existence of solutions to (3.13). Hence, we have that the solution of the stationary Mean Field equation is given by (3.8) provided (3.10) is satisfied, otherwise it is given by (3.11).

3.2. Numerical verification of the Mean Field prediction

We now test numerically how accurate is the Mean Field prediction of the stationary density profile. To measure experimentally such a profile we proceed as follows. We chose two numbers $1 \ll t_{\text{term}} \ll t_{\text{max}}$ that are called, respectively, *termalization* and *maximal* time. As an estimator for the density $\varrho(z_2)$ we use

$$\frac{1}{L_1} \frac{1}{t_{\text{max}} - t_{\text{term}} + 1} \sum_{s=t_{\text{term}}+1}^{t_{\text{max}}} \sum_{i=1}^{n(s)} \mathbb{I}_{\{x_2(i,s)=z_2\}} \quad , \tag{3.14}$$

where $\mathbb{I}_{\{\text{condition}\}}$ is equal to one if the condition is true and to zero otherwise.

The termalization and maximal time are chosen *ad hoc* so that the measure is performed when the system is in the stationary state and so that the measure is sufficiently stable.

We choose the geometrical parameters $L_1 = 100$ and $L_2 = 200$ and the probabilistic one $h = 1/2$. Then we vary the remaining ones according to the following four cases:

(i) $\varrho_u = 1$, $\varrho_d = 0$, and $\delta = 0.008$: the mean field solution is given by (3.8) with $c = -0.007887$;

(ii) $\varrho_u = 1$, $\varrho_d = 0$, and $\delta = 0.8$: the mean field solution is given by (3.8) with $c = -0.400149$;

(iii) $\varrho_u = 0.8$, $\varrho_d = 0.55$, and $\delta = 0.008$: since the first term of inequality (3.10) is equal to 5.18242, the mean field solution is given by (3.8) with $c = -0.00478572$;

(iv) $\varrho_u = 0.8$, $\varrho_d = 0.55$, and $\delta = 0.8$: since the first term of inequality (3.10) is equal to 0.0518242, the mean field solution is given by (3.11) with $c = -0.396$.

The numerical simulations are performed with $t_{\text{term}} = 10^5$ and $t_{\text{max}} = 5 \times 10^5$ and the corresponding results are depicted in Figure 3.2. In all the considered cases the match between the numerical data and the Mean Field prediction is strikingly good.

3.3. Termalization time

Since the measuring of the density profile has to be performed in the stationary states, the choice of the termalization time has to be done with care. One possibility to check if the system has reached stationarity is to compare the typical number of particles entering the system through the top boundary to that of the particles exiting from the bottom.

We proceed as following: to account for the number of particle crossing the top and bottom boundaries, we let $I(t)$ be the difference between the number of particles that entered at time t through the top boundary and that of the particles that exited through the same boundary. On the other hand, let $O(t)$ be the difference between the number of particles that exited at time t through the bottom boundary and that of the particles that entered through the same boundary. Both $I(t)$ and $O(t)$ are stochastic variables that can be positive or negative. We can expect that, if a stationary state is observed, in such a state $I(t)$ and $O(t)$ will both fluctuate around the same value.

We also define two additional quantities: given the positive integer T, we let the *local ingoing and outgoing* fluxes at time t be as

$$F_T^i(t) = \frac{1}{T} \sum_{s=\max\{0, t-T\}}^{t} I(s) \quad \text{and} \quad F_T^o(t) = \frac{1}{T} \sum_{s=\max\{0, t-T\}}^{t} O(s) \ , \qquad (3.15)$$
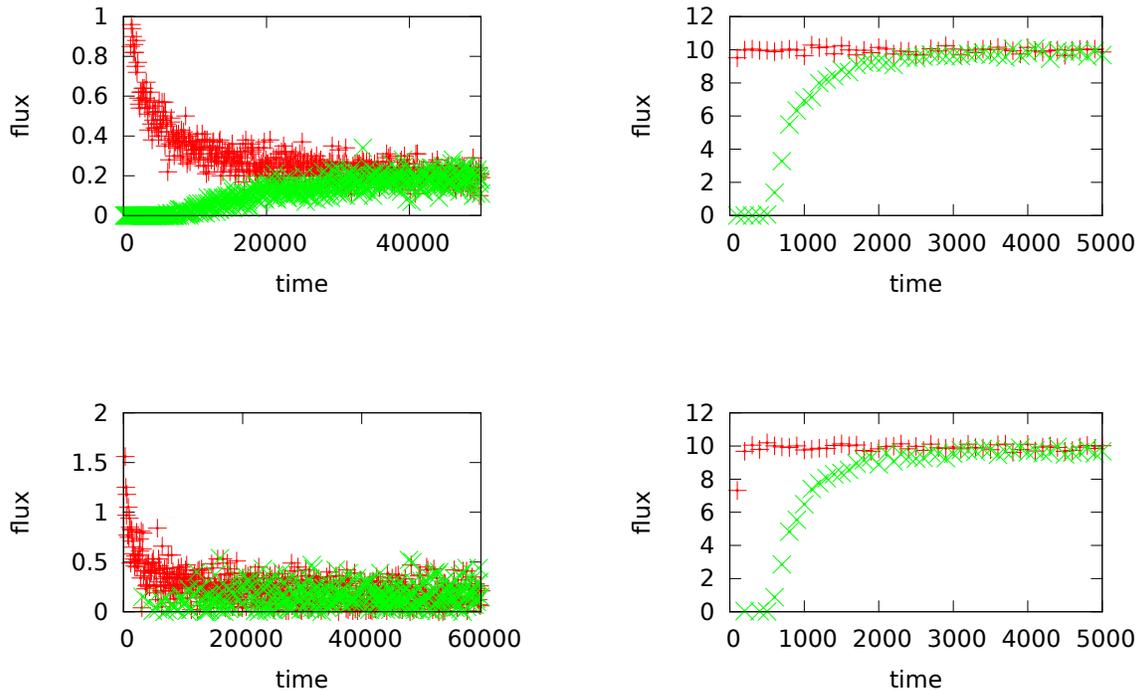
Figure 3.3: Numerical estimate of the ingoing (+) and outgoing (×) flux for the four cases described in Section 3.2: (i) top left, (ii) top right, (iii) bottom left, and (iv) bottom right.

respectively.

In Figure 3.3 we plot the local ingoing and outgoing fluxes measured on the interval $T = 100$ for the four cases (i)–(iv) considered above. The data shown in the figures indicate the choice 10^5 for the termalization time.

4. A biased birth and death model

The main physical problem we discuss in this paper is that of the typical time that (at stationarity) a particle spends in the stripe before finding its way to go out. We refer to this time as the *residence time* and we will discuss its definition in detail in the next section.

Since from this point of view only vertical displacements are relevant, we can think to the "vertical" history of the particle as to the evolution of a non–homogeneous birth and death process for the vertical coordinate with a rule depending on the stationary density profile. In this section we recall general results on this birth and death model and in the next section we discuss how to apply such results to our two–dimensional model. We mainly follow [5] for the general discussion. We derive explicit formulas in two specific simple cases, that will

turn out to be very important from the physical point of view. For the sake of completeness we outline these computations in Subsections 4.1 and 4.2.

Let L be a positive integer, $[[0, L]] := \{0, 1, \ldots, L\}$, and consider a random walk on $[[0, L]]$ with transition probabilities $p(x, y)$ with $x, y \in [[0, L]]$. We denote by $X_a(t)$, with $t = 0, 1, \ldots$ the position of the walker at time t with initial position a. We assume that at each time the walker either does not move or moves to one of the neighboring sites, i.e., we assume $p(x, y) = 0$ for $x, y \in [[0, L]]$ such that $|x - y| \geq 2$. Moreover, we let $p_x = p(x, x + 1)$ with $x = 0, \ldots, L - 1$ be the probabilities to go to the right and $q_x = p(x, x - 1)$ with $x = 1, \ldots, L$ be the probabilities to go to the left. We assume $0 \leq p_{x-1} \leq q_x < 1$ for $x = 1, \ldots, L$, namely, at each site the walker has the chance to go both to the left and to the right and the walk is left–biased. Furthermore, we assume that at least one of the "rest probabilities" $p(x, x) = 1 - (p_x + q_x)$ is different from zero so that the chain is aperiodic. We note that the more general situation in which the bias condition is removed can be treated as well, but for the sake of clearness, we shall stick to such a case.

In the case $0 < p_{x-1} \leq q_x < 1$ for $x = 1, \ldots, L$, since the birth and death process is aperiodic and positive recurrent, it has a unique invariant measure that can be written as

$$\pi(x) = \pi(0) \prod_{i=1}^{x} \frac{p_{i-1}}{q_i} \quad \text{for all } x = 1, \ldots, L \ , \tag{4.16}$$

see [5, equation (4.1)]. Note that the proof of the above statement is immediate, since one just has to verify that the above measure satisfies the detailed balance equation $\pi(x)p(x, x+1) = \pi(x + 1)p(x + 1, x)$ for all $x = 1, \ldots, L - 1$.

In [5] the authors study in detail the properties of the first hitting time of the chain to any point of the lattice $[[0, L]]$ with any initial condition (initial position of the walker). We are interested only to the hitting time

$$T := \inf\{t \geq 1, \ X_L(t) = 0\} \ , \tag{4.17}$$

i.e., the random time that the walker started at L needs to reach the origin for the first time. The expectation of such a hitting time is given by

$$\mathbb{E}[T] = \sum_{i=1}^{L} \frac{1}{q_i \pi(i)} \sum_{j=i}^{L} \pi(j) = \frac{1}{q_L} + \sum_{i=1}^{L-1} \frac{1}{q_i} \left(1 + \sum_{j=i+1}^{L} \prod_{k=i+1}^{j} \frac{p_{k-1}}{q_k}\right) \ , \tag{4.18}$$

see [5, equation (4.3)].

The first very simple remark is that, since the velocity of the particle is bounded by one, the mean hitting time to 0 cannot be smaller than L. More precisely, by using (4.18) and recalling that $q_x < 1$ for $x = 1, \ldots, L$ we get the ballistic lower bound

$$\mathbb{E}[T] \geq L \ . \tag{4.19}$$

A natural question is under which assumptions on the bias there exists a ballistic upper bound to the first hitting time to zero. We prove this bound in a very simple case, namely, when we assume that each bond is left–biased. More precisely, we show that if there exists $0 < \eta < 1$ such that $p_{x-1}/q_x \le \eta$ for $x = 1, \ldots, L$, then

$$\mathbb{E}[T] \le \frac{L}{\underline{q}(1 - \eta)} \tag{4.20}$$

where we have let $\underline{q} = \min\{q_1, \ldots, q_L\}$. Indeed, from (4.18) we have that

$$\mathbb{E}[T] \le \frac{1}{\underline{q}} + \sum_{i=1}^{L-1} \frac{1}{\underline{q}} \left(1 + \sum_{j=i+1}^{L} \prod_{k=i+1}^{j} \eta \right) = \frac{1}{\underline{q}} + \frac{1}{\underline{q}} \sum_{i=1}^{L-1} \sum_{k=0}^{L-i} \eta^k \le \frac{1}{\underline{q}} + \frac{1}{\underline{q}} \sum_{i=1}^{L-1} \sum_{k=0}^{\infty} \eta^k$$

where we have omitted few simple steps. The statement (4.20) follows recalling that $\eta < 1$.

Finally, we remark that using equations (4.16) and (4.18) we can compute the expected value of the first hitting time T. In practice this is explicitly feasible only for some particularly easy choices of the probabilities p_x and q_x. In the next subsections we discuss two physically relevant cases.

4.1. Homogeneous case

Let $0 < p \le q < 1$ be two real numbers and assume $p_x = p$ and $q_x = q$ for all $x = 0, \ldots, L$. Note that this choice satisfies all the basic assumptions on the birth and death chain.

To compute the expected value of the first hitting time T it is convenient to set $\lambda = p/q$, so that, from (4.16), we have $\pi(x) = \pi(0)\lambda^x$. Equation (4.18) yields

$$\mathbb{E}[T] = \frac{1}{q} \sum_{i=1}^{L} \frac{1}{\lambda^i} \sum_{j=i}^{L} \lambda^j = \frac{1}{q} \sum_{i=1}^{L} \sum_{j=i}^{L} \lambda^{j-i} = \frac{1}{q} \sum_{i=1}^{L} \sum_{k=0}^{L-i} \lambda^k = \frac{1}{q(1-\lambda)} \sum_{i=1}^{L} (1 - \lambda^{L-i+1}) \ .$$

By reordering the sum, we obtain

$$\mathbb{E}[T] = \frac{1}{q(1-\lambda)} \left(L - \sum_{k=1}^{L} \lambda^k \right) = \frac{1}{q(1-\lambda)} \left(L + 1 - \frac{1 - \lambda^{L+1}}{1 - \lambda} \right) = \frac{L}{q(1-\lambda)} - \frac{\lambda(1 - \lambda^L)}{q(1-\lambda)^2} \ .$$

Recalling $\lambda = p/q$, we finally have the expression

$$\mathbb{E}[T] = \frac{L}{q - p} - \frac{p}{(q-p)^2} \left[1 - \left(\frac{p}{q} \right)^L \right] \ . \tag{4.21}$$

A physical comment is useful: if $p/q < 1$, the behavior of the mean first hitting time on L is ballistic. On the other hand, we can prove that

$$\lim_{p \to q} \mathbb{E}[T] = \frac{L(L+1)}{2q}$$

Hence, in the symmetric limiting case the diffusive dependence of the mean hitting time on the length L is found. Note that the totally asymmetric limit $p \to 0$ will be considered in Section 4.3 and the ballistic scaling will be found.

4.2. A linear case

We now consider a case in which the transition probabilities q_x and p_x decrease linearly in the interval $[[0, L]]$. The physical interest of the peculiar choice we shall do will be clear in the next section. Let $A > 0$ and take

$$q_x = 2A + A(L - x) \quad \text{and} \quad p_x = A(L - x) \ . \tag{4.22}$$

By using (4.16) for the stationary measure, we find that

$$\pi(x) = \pi(0) \frac{L}{L+1} \frac{L-1}{L} \frac{L-2}{L-1} \cdots\cdots \frac{L-x+1}{L-x+2} = \pi(0) \frac{L-x+1}{L+1} \ .$$

By (4.18), we get

$$\mathbb{E}[T] = \frac{1}{A} \sum_{i=1}^{L} \frac{1}{L+2-i} \frac{1}{L+1-i} \sum_{j=i}^{L} (L+1-j) \ .$$

Since, it holds that

$$\sum_{j=i}^{L} (L+1-j) = \frac{1}{2}(L+2-i)(L-i+1) \ ,$$

we finally get

$$\mathbb{E}[T] = \frac{L}{2A} \ . \tag{4.23}$$

It is worth noting that, if A is a constant then the scaling is ballistic. But if A is small with L, then we can possibly expect to have a diffusive scaling.

4.3. The totally asymmetric case

A situation that will be useful in our discussion and that is not included in the results discussed above is the case $0 = p_{x-1} < q_x < 1$ for $x = 1, \ldots, L$, which we refer as the *totally asymmetric* case. In such a case, by using the same strategy of proof as in [5], it is easy to show that

$$\mathbb{E}[T] = \sum_{i=1}^{L} \frac{1}{q_i} \ . \tag{4.24}$$

The dependence of the mean hitting time to zero on the length of the system is, in this case, trivially ballistic. Indeed, from (4.24) we get the bounds

$$\mathbb{E}[T] \geq \frac{L}{\bar{q}} \quad \text{and} \quad \mathbb{E}[T] \leq \frac{L}{\underline{q}} \ , \tag{4.25}$$

where we have set $\underline{q} = \min\{q_1, \ldots, q_L\}$ and $\bar{q} = \max\{q_1, \ldots, q_L\}$. Note that in the totally asymmetric homogeneous case, that is to say, $0 < q_x = q < 1$ for $x = 1, \ldots, L$, we get $\mathbb{E}[T] = L/q$.

5. Residence time at stationarity

The main question we pose in this paper is to find estimates for the typical time spent by a particle in the stripe before exiting through the bottom boundary.

To give a precise definition of such a time for the simple exclusion model on the stripe defined in Section 2 we set $\varrho_{\mathrm{u}} = 1$ so that particles cannot exit the stripe through the top boundary. Once the stationary state is reached, we look at the particles that enter from the top boundary and exit from the bottom one. We count after how many steps of the dynamics the particle exits from the bottom boundary and call *residence time* the average of such a time over all the particles entered in the system after the stationary state is reached. Note that, at each step of the dynamics, a number of particles equal to the number of particles in the system at the end of the preceding time step is tentatively moved.

Despite its evident physical interest, the residence time is quite a difficult object to treat mathematically, Nevertheless, recall that, at stationarity, the average density profile is given by a function that we have denoted by $\varrho(z_2)$. Making a thought experiment, imagine that a new particle is injected into the stationary system through the top boundary. To estimate the typical time this particle needs to find its way out through the bottom boundary we note that only vertical displacements are relevant. Moreover, we can think to the "vertical" history of the particle as to the evolution of the not homogeneous birth and death process defined in Section 4 with the peculiar choice of the jump probabilities p_x and q_x that will be discussed below. We let $L = L_2$ and imagine that the value $x = 0$ of the birth and death process represents the particle at the row $L_2 + 1$ of the lattice (bottom boundary), the value $x = L_2$ represents the particle at the row 1 of the lattice (the row close to the top boundary), and the generic value x represents the particle at the row $L_2 + 1 - x$ of the lattice. The only not zero transition probabilities of the birth and death process are chosen as

$$
\begin{cases}
q_x = \dfrac{1-h}{2}(1+\delta)[1 - \varrho(L_2 + 1 - x + 1)] & \text{for } x = 1, \ldots, L_2 \\[4mm]
p_x = \dfrac{1-h}{2}(1-\delta)[1 - \varrho(L_2 + 1 - x - 1)] & \text{for } x = 0, \ldots, L_2 - 1
\end{cases}
\tag{5.26}
$$

Indeed, recalling the expressions (3.2) for the probabilities u and d, the prefactor $(1-h)(1+\delta)/2$ in the expression of q_x is nothing but the probability d to move the particle in the real space downwards; while the second factor is nothing but the probability that, at stationarity,

the site where the particle tries to jump is empty. The expression for p_x can be justified similarly. Note that the birth and death process has a rest probability $1 - (p_x + q_x)$ different from zero, this is due to the fact that the real particle can also not move or move horizontally.

We now propose a conjecture for the residence time of the exclusion model and we will test it numerically in the next section.

Conjecture *The residence time[1] of the model introduced in Section 2 is equal to the mean value of the first hitting time to* 0 *for the birth and death process started at* L_2.

The main properties of birth and death processes have been recalled in Section 4. Those results and the conjecture above suggest that, for $\delta < 1$, the residence time is given by equation (4.18) where the stationary measure π is given by (4.16) with the jump probabilities p_i and q_i defined in (5.26). Since the stationary density profile is given with great accuracy by the stationary Mean Field equation, we can use these equations to give an estimate of the residence time of the model. It is worth noting that, since the expression of the stationary density profile is rather complicated, see (3.8) and (3.11), it will not be possible to derive in general explicit formulas for the residence time. On the other hand, since in (4.18) and (4.16) only finite product and sums are involved, we will be able to compute estimates for the residence time numerically for any values of the parameters of the model. In the case $\delta = 1$ the expression (4.24) should be used.

Let us now discuss three simple cases in which explicit expressions of the residence time can be derived explicitly.

5.1. Totally vertically asymmetric model

Recall we assumed $\varrho_{\mathrm{u}} = 1$. Consider, more, the case $\delta = 1$. From the profiles in Figure 3.2 (graphs on the right) it is rather clear that in this situation the density profile is with very good approximation constant throughout the stripe.

Denote by $\bar{\varrho}$ such a constant value of the density profile. By (5.26), it follows that the birth and death model has the jump probabilities

$$q_x = (1 - h)(1 - \bar{\varrho}) \ \ x = 1, \ldots, L_2 \quad \text{and} \quad p_x = 0 \ \ x = 0, \ldots, L_2 - 1$$

---

[1]Since in the real model a particle at the fictitious row $L_2 + 1$ cannot jump back to the real row L_2, one should set the probability $p(0,1) = 0$. This would be a problem for the birth and death process, where all the jumping probabilities has to be assumed strictly positive, but for our purpose it is not necessary, since we are only interested to the first hitting time to 0, so that when the one dimensional birth and death process reaches such a state it is stopped. Hence all our results will not depend on the choice of the probability $p(0,1)$.

Hence, by the results in Section 4.3, we have that the residence time is given by

$$R = \frac{L_2}{(1-h)(1-\bar{\varrho})} \ . \tag{5.27}$$

In particular, the large L_2 behavior of the residence time given by (5.27) is ballistic with a slope depending on the parameters h and $\bar{\varrho}$.

5.2. Large drift case

Recall we assumed $\varrho_\mathrm{u} = 1$. Consider δ close to one. From the profiles in Figure 3.2 (graphs on the right) it is rather clear that in this situation the density profile is with very good approximation equal to a constant, denoted again by $\bar{\varrho}$. By (5.26) it follows that the birth and death model has the jump probabilities

$$q_x = \frac{1-h}{2}(1+\delta)(1-\bar{\varrho}) \ \ x=1,\ldots,L_2 \quad \text{and} \quad p_x = \frac{1-h}{2}(1-\delta)(1-\bar{\varrho}) \ \ x=0,\ldots,L_2-1$$

Hence, by (4.21), we have that the residence time is given by

$$R = \frac{L_2}{(1-h)(1-\bar{\varrho})\delta} - \frac{1-\delta}{2(1-h)(1-\bar{\varrho})\delta^2}\left[1-\left(\frac{1-\delta}{1+\delta}\right)^{L_2}\right] \ . \tag{5.28}$$

The formula (5.28) suggests that in this case the dependence of the residence time on L_2 is ballistic, but this statement needs more care. Indeed, the equation above is based on the assumption that the density profile is constant with good approximation in this regime and such an assumption is based on the results obtained via the Mean Field equation. But we have to recall that the Mean Field equation has been (not rigorously) derived in the large volume limit with the drift parameter scaling to zero with L_2. For this reason it is not correct, in principle, to fix δ and let $L_2 \to \infty$ in the above formula.

We remark, that in this case we shall as well be able to deduce the ballistic scaling of the residence time with L_2 in Section 5.4 via a different argument.

5.3. Zero drift

Consider, now, the case $\delta = 0$ (zero drift) again for $\varrho_\mathrm{u} = 1$. In the absence of drift the stationary density profile is linear, hence

$$\varrho(x) = 1 - \frac{1-\varrho_\mathrm{d}}{L_2+1}x \tag{5.29}$$

for $x = 0, \ldots, L_2+1$. By (5.26), we get also that

$$q_x = \frac{1-h}{2}\frac{1-\varrho_\mathrm{d}}{L_2+1}(L_2+2-x) \quad \text{and} \quad p_x = \frac{1-h}{2}\frac{1-\varrho_\mathrm{d}}{L_2+1}(L_2-x) \ .$$

Thus, by using the result (4.23) from Section 4.2, we find the residence time

$$R = \frac{L_2(L_2 + 1)}{(1 - h)(1 - \varrho_{\rm d})} \; . \tag{5.30}$$

As expected, the large volume ($L_2 \to \infty$) behavior of the residence time is quadratic in the purely diffusive zero drift case.

5.4. Dependence of the residence time on the length of the stripe

In this section we focus on the dependence of the residence time on the length L_2 of the stripe. We expect that for $\delta > 0$, since there is a preferred direction in the movement, the particles will have a not zero average vertical velocity. As a consequence, we expect a ballistic behavior and a linear dependence of the residence time on L_2.

We have already shown in Section 5.1 that this is indeed the case for $\delta = 1$. Assume, now, that the drift δ is fixed and $0 < \delta < 1$. From (5.26), we see

$$\frac{p_{x-1}}{q_x} = \frac{1 - \delta}{1 + \delta} \frac{1 - \varrho(L_2 + 1 - x)}{1 - \varrho(L_2 + 1 - x + 1)}$$

for any $x = 1, \ldots, L_2$. Since, $\varrho_{\rm u} = 1 > \varrho_{\rm d} \geq 0$ we can reasonably assume that the density profile is a decreasing function of the vertical spatial coordinate. Thus, $\varrho(L_2 + 1 - x) > \varrho(L_2 + 1 - x + 1)$ implies that there exists $\eta < 1$ such that $p_{x-1}/q_x \leq \eta$. This remark and (4.20) ensure that, for any positive finite δ, the residence time has a ballistic dependence on the length of the stripe.

Finally, for $\delta = 0$ we have shown in Section 5.3, cf. (5.30), that the residence time is quadratic in L_2 (diffusive scaling). We stress that this result is not trivial at all. Indeed, even in the case $\delta = 0$ the birth and death model that we use to investigate the property of the residence time is not symmetric. The lack of symmetry is due to

$$q_x - p_{x-1} = \frac{1 - h}{2} \frac{1 - \varrho_{\rm d}}{L_2 + 1}$$

for any $x = 1, \ldots, L_2$. The diffusive scaling is a consequence of the fact that this difference vanishes as $1/(L_2 + 1)$.

5.5. Single file regime

The model we study is two–dimensional. Particles move in a stripe from the top boundary towards the bottom one due to the presence of a drift δ or just because of a vertical biased diffusion due to the difference between the boundary densities on the top and on the bottom end of the stripe. The particles are subjected also to horizontal displacements whose probability is controlled by the parameter h.

In the particular case $h = 0$, our model becomes one–dimensional and particles move, each on its vertical line, as in a single file system. In other words in this case our model reduces to the one–dimensional simple exclusion model with open boundaries. The specification "open boundaries" means that the system is finite and at the boundaries there is a rule prescribing the rate at which particles can either enter or leave the system.

This model has been widely studied, see for instance [11] for the seminal paper where the model was solved exactly in the totally asymmetric case. See, also, [8] for a general review. Our results can be compared easily to those in [11] which refer to the totally asymmetric case, namely, for our case $\delta = 1$. In [11] one computes the stationary current J, namely, the number of particles that for unit of time crosses one bond at stationarity. With our notation one finds

$$J = \begin{cases} 1/4 & \text{for } \varrho_{\mathrm{d}} \leq 1/2 \\ \varrho_{\mathrm{d}}(1 - \varrho_{\mathrm{d}}) & \text{for } \varrho_{\mathrm{d}} > 1/2 \end{cases} \tag{5.31}$$

in the case $\varrho_{\mathrm{u}} = 1$ (see [11, equations (58) and (60)]).

Now, since in the totally asymmetric case the stationary density throughout the system is equal to a constant $\bar{\varrho}$, we can write $J \approx \bar{\varrho} L_2 / \mathbb{E}[T]$. Hence, we have that

$$\mathbb{E}[T] \approx \bar{\varrho} \, \frac{L_2}{J}$$

which reduces to our result (5.27) with $h = 0$ once we use (5.31) and notice that $\bar{\varrho} = 1/2$ for $\varrho_{\mathrm{d}} \leq 1/2$ and $\bar{\varrho} = \varrho_{\mathrm{d}}$ for $\varrho_{\mathrm{d}} > 1/2$.

Additionally, we mention here an interesting result which is valid for the symmetric simple exclusion model in dimension one on the whole line (no boundary). In both [15] and [13], the authors compute the variance of the position of a tagged particle and they prove that it is proportional to the square root of time, meaning that the typical distance spanned by the (symmetric) walker is proportional to $t^{1/4}$. In our problem we do not find any L_2^4 scaling for the residence time even in the single–file regime. Indeed, we think that there is no direct connection between the two problems. One important point is that the results in [13, 15] deal with a simple exclusion model without drift (symmetric) and without boundaries. In our problem, even in the zero drift ($\delta = 0$) case, a net flux is present due to the boundary conditions.

6. Numerical estimates of the residence time

In this section we test numerically the validity of the conjecture on the residence time proposed in Section 5. We choose the parameters of the model as follows: take $\varrho_{\mathrm{u}} = 1$, $L_1 = 100$, and consider the cases

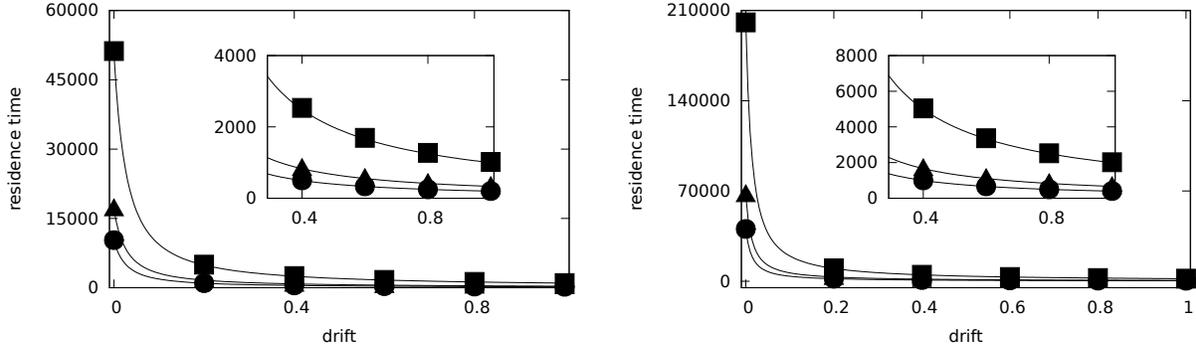$$L_2 = 100, 200, \quad \delta = 0, 0.2, 0.4, 0.6, 0.8, 1, \quad \varrho_{\mathrm{d}} = 0, 0.4, 0.8, \quad h = 0, 0.4, 0.8.$$

Figure 6.4: Residence time versus drift in the cases $\varrho_{\mathrm{d}} = 0$ and $L_2 = 100$ (left) and $L_2 = 200$ (right). The symbols ●, ▲, and ■ refer, respectively, to the cases $h = 0, 0.4, 0.8$. The inset in the left picture is just a zoom of part of the data of the same picture. Solid lines are the theoretical prediction.

In all these cases, the residence time has been evaluated by averaging over all the particles entered in the system through the top boundary after the time t_{term}, namely, at stationarity, and exited through the bottom one at a time smaller than $t_{\max}$. The simulations have been performed with $t_{\mathrm{term}} = 5 \times 10^5$ and $t_{\max} = 5 \times 10^6$.

To check the dependence of the residence time on the length of the stripe we had to consider a few more cases with larger L_2, viz. $L_2 = 300, 400$, $\delta = 0, 0.4, 1$, $\varrho_{\mathrm{d}} = 0$, and $h = 0.4$. In these cases, due to the length of the stripe, we had to use $t_{\mathrm{term}} = 10^6$ and $t_{\max} = 2 \times 10^7$.

The numerical estimates of the residence time with the associated statistical error (the standard deviation divided times the square root of the number of measures) are reported in Appendix A. In all the pictures the vertical bar representing the statistical error is not visible since it is smaller than the symbol representing the measured value of the residence time.

We compare the numerical results with the theoretical prediction. In general the theoretical prediction of the residence time is the value given by (4.18) with the stationary measure π given by (4.16) where the jump probabilities p_i and q_i are defined in (5.26). Since we could not derive explicit expressions in terms of the model parameters, the theoretical prediction has been computed by performing sums and products numerically. In the case $\delta = 1$ (see for instance the discussion in Section 6.2) the theoretical prediction is the value given by (4.24) with the q_i's defined in (5.26). In the case $\delta = 0$ (see for instance the discussion in Section 6.3) the theoretical prediction is given explicitly by (5.30).

We find that the match between the theoretical prediction based on the birth and death model and the numerical data is perfect for any choice of the parameters of the model
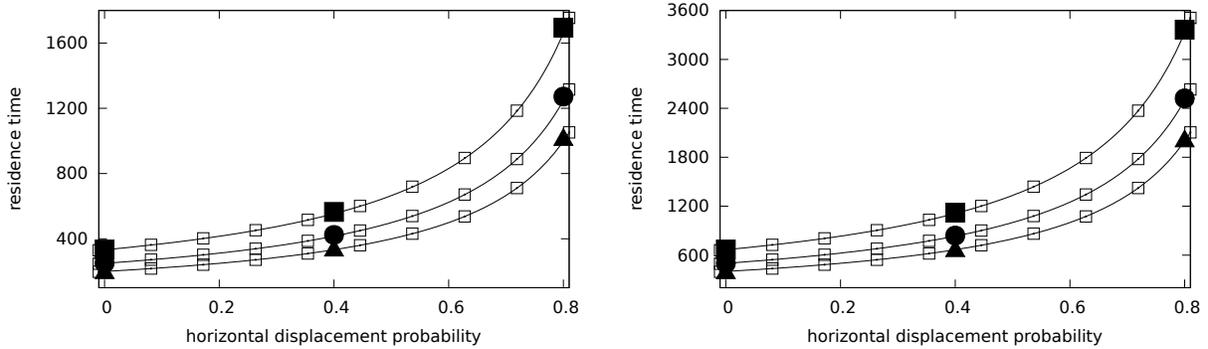
Figure 6.5: Residence time versus the horizontal displacement probability h in the cases $\varrho_d = 0$ and $L_2 = 100$ (left) and $L_2 = 200$ (right). The symbols ■, •, and ▲ refer, respectively, to the cases $\delta = 0.6, 0.8, 1$. Data referring to the cases $\delta = 0, 0.2, 0.4$ are reported in Appendix A, but not plotted in the picture, since they would be out of scale. Solid lines are the theoretical prediction. Open squares are the approximated theoretical prediction (5.28) with $\bar{\varrho} = 1/2$, which is valid in the large drift regime.

provided either $\varrho_d = 0$ or $\delta = 1$ (or both). To illustrate this fact we first discuss our data at $\varrho_d = 0$ ant let $h = 0, 0.4, 0.8$ and $\delta = 0, 0.2, 0.4, 0.6, 0.8, 1$. Then, we consider $\delta = 1$ and let $h = 0, 0.4, 0.8$ and $\varrho_d = 0, 0.4, 0.8$.

Finally, for the region where the match between the theoretical prediction and the numerical results is not good, we consider the worst case from the point of view of drift, namely, we choose $\delta = 0$ and let, again, $h = 0, 0.4, 0.8$ and $\varrho_d = 0, 0.4, 0.8$. We shall notice that the match between theory and experiment, even if qualitatively correct, is quantitave worst and worst when ϱ_d is increased. But, we shall also remark that, fixed ϱ_d, the match is better at larger values of the horizontal displacement probability h.

The physical interpretation of this fact is that at large ϱ_d and drift $\delta < 1$ particles accumulates close to the bottom exit and, due to bouncing back of particles, fluctuations are not more negligible. For this reason our theoretical prediction, which is based only on the stationary shape of the density profile, is not anymore efficient.

6.1. Case $\varrho_d = 0$

We discuss first the case $\varrho_d = 0$ and show that here the theoretical prediction of the residence time based on the birth and death model discussed in Section 5 agrees perfectly with the numerical results.

In Figure 6.4 it is shown the dependence of the residence time on the drift δ for $\varrho_d = 0$ and for different values of the horizontal displacement probability h. The dependence of the residence time on the horizontal displacement probability for different values of the drift is shown in Figure 6.5.
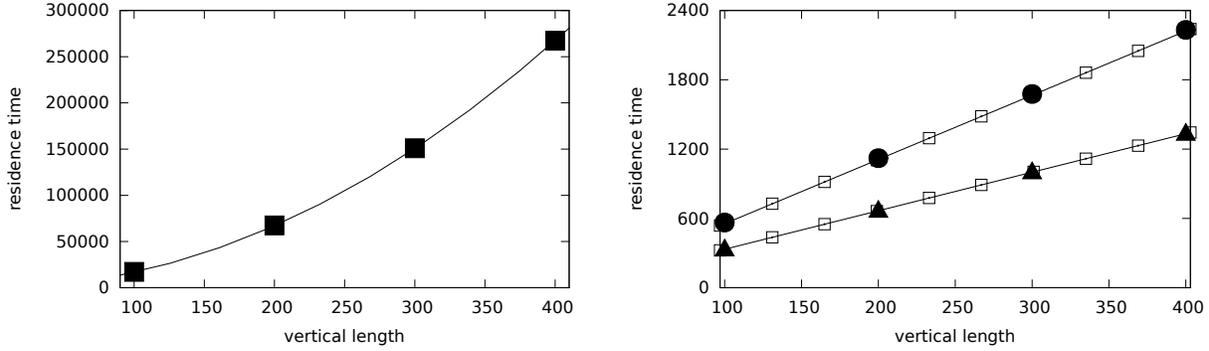
Figure 6.6: Residence time versus length of the stripe L_2 in the case $\varrho_{\mathrm{d}} = 0$ and $h = 0.4$. The symbol ■ refers to the case $\delta = 0$ (left picture) while the symbols • and ▲ refer, respectively, to the cases $\delta = 0.8, 1$. Solid lines are the theoretical prediction; in the picture in the left the explicit expression (5.30) is used, Open squares are the approximated theoretical prediction (5.28) with $\bar{\varrho} = 1/2$, which is valid in the large drift regime.

The fact that the residence time decreases with the drift and increases with the horizontal displacement probability is completely reasonable. The match between the simulation data and the theoretical prediction is perfect. It is remarkable the fact that even the approximated expression (5.28) (which in the case $\delta = 1$ reduces to (5.27)) gives a perfect estimate of the residence time. This is due to the fact that for the values of the parameter that we have chosen the stationary density profile throughout the system is constantly equal to $1/2$ with very a good approximation.

In Figure 6.6, the residence time in the case ϱ_{d} has been plotted as a function of the length L_2 of the stripe for different values of the drift and for $h = 0.4$. It is remarkable to note the striking match between theory and simulation. In particular the fact that the behavior is linear (ballistic) for $\delta > 0$ and quadratic (diffusive) for $\delta = 0$, see the theoretical discussion in Section 5.4, is confirmed by the numerical experiment.

6.2. Case $\delta = 1$

This is the case of totally asymmetric simple exclusion rule along the vertical direction. Here, particles can never jump upwards. We show that, for this scenario, the theoretical prediction of the residence time based on the birth and death model discussed in Section 5 agrees perfectly with the numerical results.

We show three pictures: the dependence of the residence time on the horizontal displacement probability h (Figure 6.7), the dependence on the bottom boundary density ϱ_{d} (Figure 6.8), and, finally, the dependence on the length of the stripe L_2 (Figure 6.9).

We do not repeat the discussion in detail. We just mention that the linearity of the residence time with respect to the length of the stripe is confirmed by the experimental data
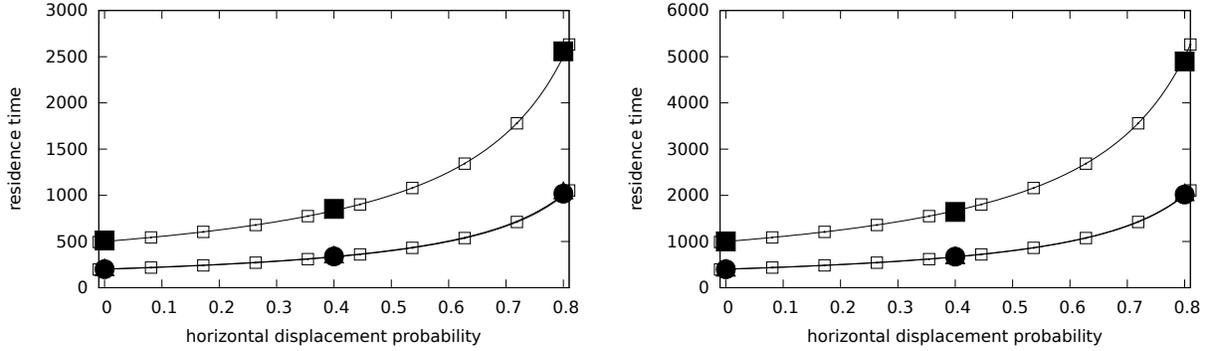
Figure 6.7: Residence time versus the horizontal displacement probability h in the cases $\delta = 1$ and $L_2 = 100$ (left) and $L_2 = 200$ (right). The symbols •, ▲, and ■ refer, respectively, to the cases $\varrho_d = 0, 0.4, 0.8$. Note that bullets and black triangle are perfectly coinciding, this is due to the fact that in this regime the residence time does not depend that much on the bottom boundary density, provided it is smaller that $1/2$. In such a case, indeed, the density profile inside the stripe is almost perfectly constant and equal to $1/2$. Solid lines are the theoretical prediction. Open squares are the approximated theoretical prediction (5.28) valid in the large drift regime with $\bar{\varrho} = 1/2$ for the cases $\varrho_d = 0, 0.4$ and with $\bar{\varrho} = 8/10$ in the case $\varrho_d = 0.8$. Indeed, in the first two cases the density profile is almost constantly equal to $1/2$, while in the last case it is almost constantly equal to $8/10$.

and refer the reader to the caption of the pictures for more specific comments.

6.3. Case $\delta = 0$

We discuss now the case of a symmetric simple exclusion rule along the vertical direction. As we already mentioned at the beginning of this section, in this case the match between the theoretical prediction and the numerical data is only qualitatively good. More precisely, the theoretical prediction of the residence time based on the birth and death model discussed in Section 5 agrees perfectly with the numerical results for $\varrho_d = 0$ (see also Section 6.1), whereas the agreement is only qualitative for $\varrho_d > 0$ and it is quantitatively worse and worse when ϱ_d is chosen closer and closer to 1.

We show three pictures: the dependence of the residence time on the horizontal displacement probability h (Figure 6.10), the dependence on the bottom boundary density ϱ_d (Figure 6.11), and, finally, the dependence on the length of the stripe L_2 (Figure 6.12).

Note that in this section, since $\delta = 0$, the theoretical prediction is given by the explicit formula (5.30).

The relevant comment now is that the match between theory and experiment is improved provided the horizontal displacement probability is increased. As explained at the end of the paragraph opening this section this phenomenon can be explained via two mechanisms: bouncing back and the possibility to bypass clusters of blocking particles. The former sug-
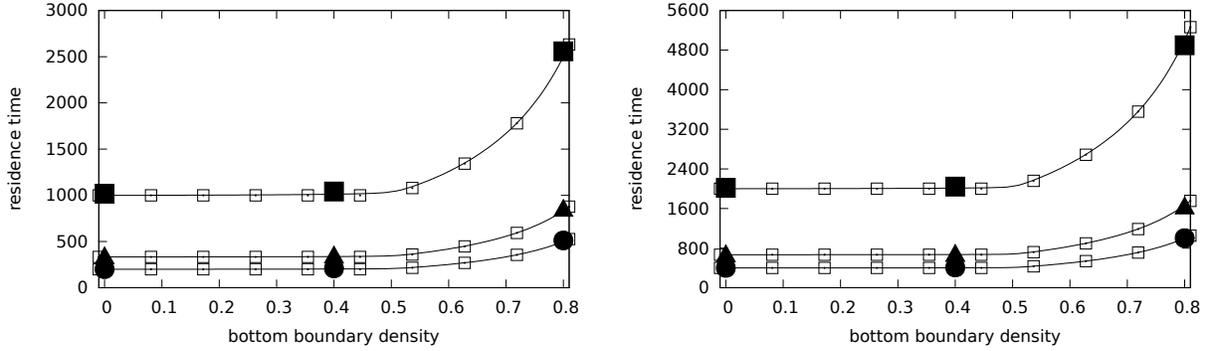
Figure 6.8: Residence time versus the bottom boundary density ϱ_{d} in the cases $\delta = 1$ and $L_2 = 100$ (left) and $L_2 = 200$ (right). The symbols •, ▲, and ■ refer, respectively, to the cases $h = 0, 0.4, 0.8$. Solid lines are the theoretical prediction. Open squares are the approximated theoretical prediction (5.28) valid in the large drift regime with $\bar{\varrho} = 1/2$ for $\varrho_{\mathrm{d}} \leq 1/2$ and with $\bar{\varrho} = \varrho_{\mathrm{d}}$ for $\varrho_{\mathrm{d}} > 1/2$. Indeed, when $\varrho_{\mathrm{d}} < 1/2$ the density profile is almost constantly equal to $1/2$, while for $\varrho_{\mathrm{d}} > 1/2$ it is almost constantly equal to ϱ_{d}.

gests that correlations become important in this regime so that a model based only on the average stationary density profile cannot explain the behavior of the system. On the other hand, the latter phenomenon suggests that the effect of bouncing back is milder when the horizontal displacement probability is larger, since particles have a good chance to avoid blocking clusters.

6.4. Non–monotonic behavior in the bouncing back regime

As it has been seen in the previous section the residence time is typically an increasing function of the horizontal displacement probability. This is an obvious fact. Indeed, when h is increased particles spend a lot of time in performing horizontal jumps which are a waste of time in the run towards the bottom exit.

In this section we show that in the regime in which the bouncing back phenomenon is present a small not zero horizontal probability displacement can favour the exit of the particles.

We have performed the following simulations: $\varrho_{\mathrm{u}} = 1$ (as always), $L_1 = 100$, $L_2 = 200$, $\delta = 0$,

$$\varrho_{\mathrm{d}} = 0, 0.2, 0.4, 0.6, 0.8, \qquad \text{and} \quad h = 0, 0.01, 0.02, \ldots, 0.10 \ .$$

As before, in all these cases, the residence time has been evaluated by averaging over all the particles entered in the system through the top boundary after the time t_{term}, namely, at stationarity, and exited through the bottom one at a time smaller than t_{max}. The simulations have been performed with $t_{\mathrm{term}} = 5 \times 10^5$ and $t_{\mathrm{max}} = 5 \times 10^6$. The numerical estimates of the
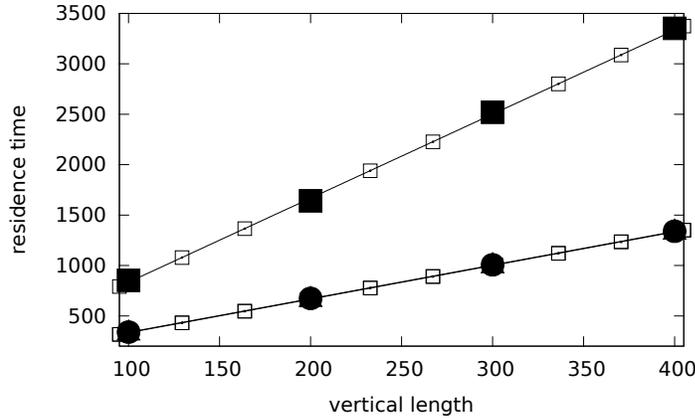
Figure 6.9: Residence time versus the vertical length of the stripe L_2 in the case $\delta = 1$ and $h = 0.4$. The symbols •, ▲, and ■ refer, respectively, to the cases $\varrho_d = 0, 0.4, 0.8$. Note that bullets and black triangle are perfectly coinciding, this is due to the fact that in this regime the residence time does not depend that much on the bottom boundary density, provided it is smaller that $1/2$. In such a case, indeed, the density profile inside the stripe is almost perfectly constant and equal to $1/2$. Solid lines are the theoretical prediction. Open squares are the approximated theoretical prediction (5.28) valid in the large drift regime with $\bar{\varrho} = 1/2$ for the cases $\varrho_d = 0, 0.4$ and with $\bar{\varrho} = 8/10$ in the case $\varrho_d = 0.8$. Indeed, in the first two cases the density profile is almost constantly equal to $1/2$, while in the last case it is almost constantly equal to $8/10$.

residence time, with the associated statistical error (the standard deviation divided times the square root of the number of measures), are reported in Appendix B.

In Figure 6.13, the residence time is plotted as function of the horizontal displacement probability. It is remarkable the presence of a minimum at small values of h. This fact can be interpreted as follows: in the bouncing back regime, namely, when ϱ_d is high and δ low, a particle can find a blocking cluster of particles in its way out through the bottom boundary. In such a situation, then, having a larger horizontal displacement probability can help the particle to bypass the obstacle. Obviously, if h is increased too much this effect disappears due to the time wasted by the particles in horizontal movements.

7. Conclusions

We focused our attention on the study of the simplest two–dimensional model that mimics the flow of particles in a straight pipe under the effect of different driving boundary conditions and external fields. We studied the residence time, i.e., the typical time a particle entering the stripe at stationarity from the top boundary needs to exit through the bottom one, under the assumption that particles in the stripe interact only via hard–core exclusion and vertical boundaries are reflecting.
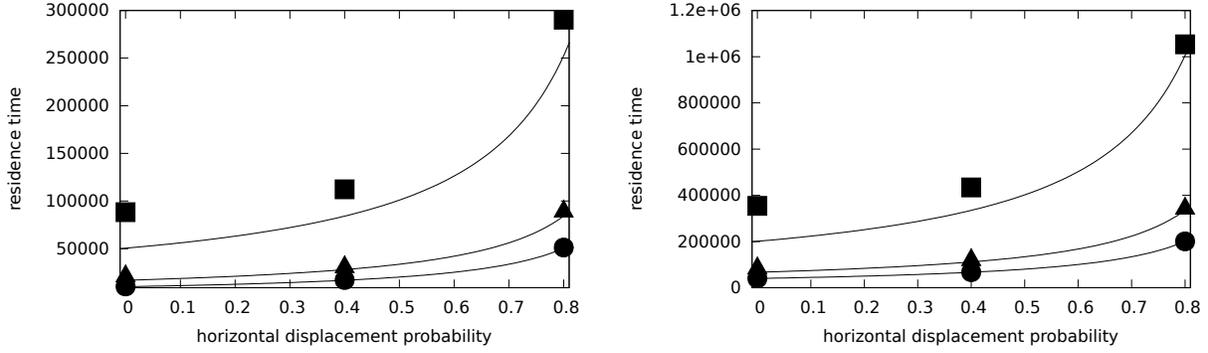
Figure 6.10: Residence time versus the horizontal displacement probability h in the cases $\delta = 0$ and $L_2 = 100$ (left) and $L_2 = 200$ (right). The symbols $\bullet$, $\blacktriangle$, and $\blacksquare$ refer, respectively, to the cases $\varrho_{\mathrm{d}} = 0, 0.4, 0.8$. Solid lines are the theoretical prediction (5.30).
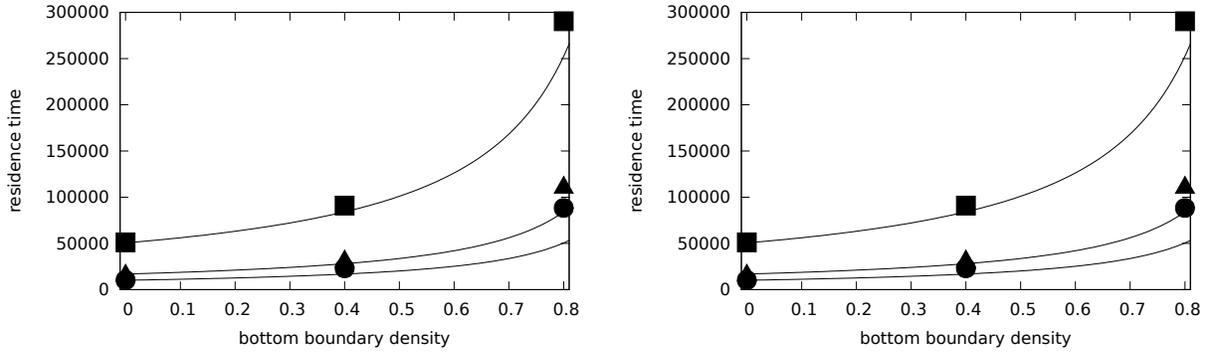
Figure 6.11: Residence time versus the bottom boundary density ϱ_{d} in the cases $\delta = 0$ and $L_2 = 100$ (left) and $L_2 = 200$ (right). The symbols $\bullet$, $\blacktriangle$, and $\blacksquare$ refer, respectively, to the cases $h = 0, 0.4, 0.8$. Solid lines are the theoretical prediction (5.30).

We explored the dependence of the residence time on the external driving force, length of the stripe, horizontal diffusion, and boundary conditions. We have shown that, in almost all the considered regimes, the mean residence time is equal to the average time needed to cross the stripe by a particle performing a random walk in a background prescribed by the stationary density profile of the original model. In this way, in particular, we recover the structure of the fluxes as well as the residence times proven mathematically in dimension one in [11].

This picture fails to be correct in the case in which there is a particle accumulation close to the bottom boundary (exit). In this regime, we discover new effects that are consequence of the two–dimensionality of the system. The most relevant is the non–monotonic behavior in changes in the horizontal displacement probability in the bouncing back regime.

This particle accumulation situation can be realized artificially by inserting obstacles in the stripe. We then expect interesting non–linear phenomena to show up. We shall study
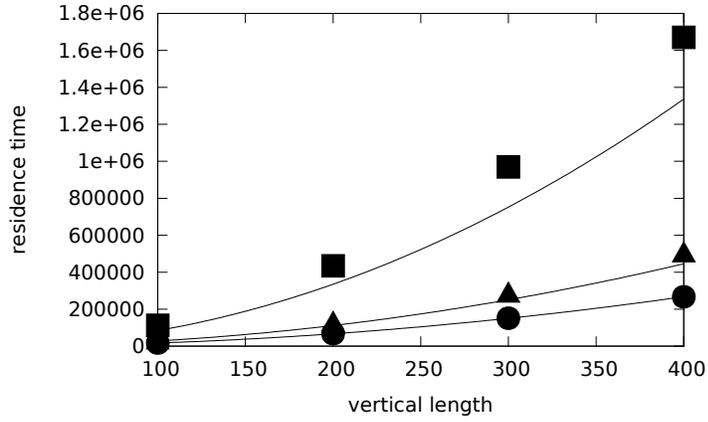
Figure 6.12: Residence time versus the vertical length of the stripe L_2 in the case $\delta = 0$ and $h = 0.4$. The symbols •, ▲, and ■ refer, respectively, to the cases $\varrho_{\mathrm{d}} = 0, 0.4, 0.8$. Solid lines are the theoretical prediction (5.30).
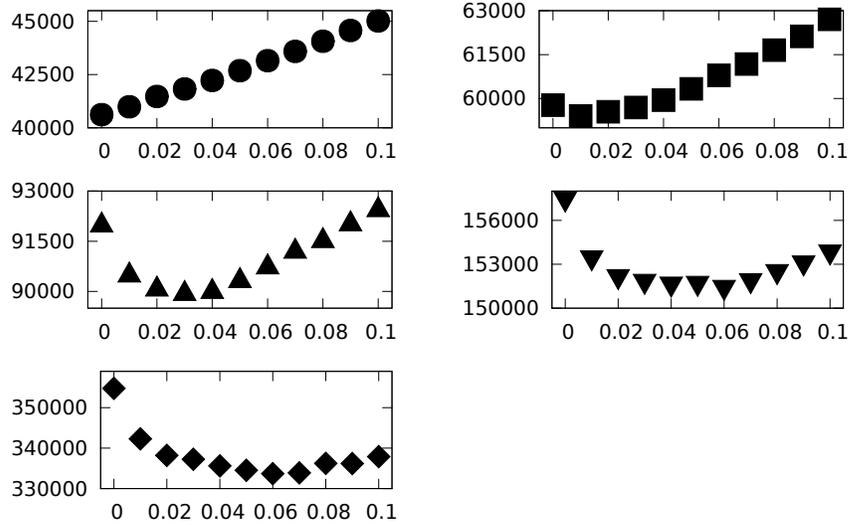
this regime in a follow–up paper.

Figure 6.13: Residence time versus the horizontal displacement probability h in the case $\delta = 0$ and $L_2 = 200$. The symbols $\bullet$, $\blacksquare$, $\blacktriangle$, $\blacktriangledown$, and $\blacklozenge$ refer, respectively, to the cases $\varrho_{\mathrm{d}} = 0, 0.2, 0.4, 0.6, 0.8$.

A. Numerical estimates

In this appendix we report the numerical values of the residence time discussed in Sections 6.1 – 6.3. In the tables we list the parameters of the simulation, the mean residence time and the associated statistical error (the standard deviation divided times the square root of the number of measures).

δ	ϱ_{d}	h	res. time $L_2 = 100$	error	res. time $L_2 = 200$	error
0.0	0.0	0.0	10296.15	0.644	40597.45	2.509
0.0	0.0	0.4	17160.13	6.923	67479.69	38.135
0.0	0.0	0.8	51216.23	41.180	200784.27	228.637
0.0	0.4	0.0	23049.45	2.108	92026.94	8.505
0.0	0.4	0.4	32522.23	17.154	127695.26	95.023
0.0	0.4	0.8	90952.27	94.934	350755.39	521.740
0.0	0.8	0.0	88370.52	14.060	354277.53	26.153
0.0	0.8	0.4	112283.28	104.664	434155.57	581.129
0.0	0.8	0.8	290364.72	534.828	1053710.03	2817.114
0.2	0.0	0.0	987.18	0.015	1995.05	0.021
0.2	0.0	0.4	1664.82	0.080	3346.76	0.117
0.2	0.0	0.8	4996.69	0.472	10048.04	0.684
0.2	0.4	0.0	1070.73	0.017	2084.21	0.022
0.2	0.4	0.4	1781.39	0.081	3466.11	0.120
0.2	0.4	0.8	5334.84	0.501	10385.07	0.704
0.2	0.8	0.0	2554.14	0.067	5029.31	0.108
0.2	0.8	0.4	4237.51	0.233	8367.71	0.327
0.2	0.8	0.8	12674.94	1.436	24878.30	1.996
0.4	0.0	0.0	500.33	0.005	1001.37	0.007
0.4	0.0	0.4	844.33	0.022	1680.55	0.031
0.4	0.0	0.8	2534.41	0.125	5040.57	0.176
0.4	0.4	0.0	527.69	0.006	1030.42	0.008
0.4	0.4	0.4	878.65	0.023	1714.87	0.031
0.4	0.4	0.8	2632.92	0.129	5141.28	0.180
0.4	0.8	0.0	1276.82	0.024	2507.51	0.044
0.4	0.8	0.4	2125.84	0.063	4144.74	0.088

0.4	0.8	0.8	6371.61	0.375	12384.38	0.513
0.6	0.0	0.0	334.52	0.003	668.04	0.004
0.6	0.0	0.4	564.51	0.010	1121.03	0.014
0.6	0.0	0.8	1694.51	0.057	3364.06	0.080
0.6	0.4	0.0	349.71	0.003	684.33	0.004
0.6	0.4	0.4	582.16	0.011	1138.49	0.015
0.6	0.4	0.8	1745.20	0.059	3413.10	0.081
0.6	0.8	0.0	851.49	0.013	1669.38	0.026
0.6	0.8	0.4	1418.99	0.031	2750.35	0.043
0.6	0.8	0.8	4257.04	0.174	8217.48	0.236
0.8	0.0	0.0	251.15	0.002	501.22	0.003
0.8	0.0	0.4	423.89	0.006	840.56	0.009
0.8	0.0	0.8	1272.07	0.033	2522.61	0.046
0.8	0.4	0.0	261.48	0.002	512.28	0.003
0.8	0.4	0.4	435.15	0.006	852.17	0.009
0.8	0.4	0.8	1304.62	0.034	2555.00	0.048
0.8	0.8	0.0	639.08	0.008	1252.55	0.017
0.8	0.8	0.4	1065.10	0.019	2056.98	0.027
0.8	0.8	0.8	3193.53	0.102	6137.87	0.140
1.0	0.0	0.0	200.98	0.001	400.92	0.002
1.0	0.0	0.4	339.22	0.004	672.87	0.006
1.0	0.0	0.8	1018.00	0.022	2017.75	0.031
1.0	0.4	0.0	208.82	0.001	409.40	0.002
1.0	0.4	0.4	347.48	0.004	680.89	0.006
1.0	0.4	0.8	1041.26	0.022	2042.36	0.031
1.0	0.8	0.0	511.72	0.006	1002.10	0.012
1.0	0.8	0.4	852.90	0.013	1641.02	0.020
1.0	0.8	0.8	2558.00	0.068	4897.61	0.094

Table 1: Numerical estimate of the residence time in the cases $L_2 = 100$ and $L_2 = 200$.

δ	ϱ_{d}	h	res. time $L_2 = 300$	error	res. time $L_2 = 400$	error
0.0	0.0	0.4	150914.75	73.70	267196.73	150.785
0.0	0.4	0.4	285468.79	182.90	503696.30	376.217
0.0	0.8	0.4	969762.10	1115.43	1670418.61	2276.871
0.6	0.0	0.4	1677.06	0.013	1339.79	0.006
1.0	0.0	0.4	1006.36	0.005	2232.36	0.014
1.0	0.4	0.4	1014.69	0.005	1347.98	0.006
1.0	0.8	0.4	2519.67	0.016	3352.54	0.018

Table 2: Numerical estimate of the residence time in the cases $L_2 = 300$ and $L_2 = 400$.

B. More numerical estimates

We report, here, the numerical values of the residence time discussed in Section 6.4. In the table we list the parameters of the simulation, the mean residence time and the associated statistical error (the standard deviation divided times the square root of the number of measures).

ϱ_{d}	h	res. time	error
0.0	0.00	40618.69	2.538
0.0	0.01	40989.47	8.610
0.0	0.02	41471.93	10.216
0.0	0.03	41825.83	11.302
0.0	0.04	42225.82	12.174
0.0	0.05	42679.64	12.953
0.0	0.06	43152.68	13.669
0.0	0.07	43585.88	14.336
0.0	0.08	44066.76	14.947
0.0	0.09	44572.55	15.554
0.0	0.10	45016.32	16.095
0.2	0.00	59773.35	4.653
0.2	0.01	59403.66	14.248
0.2	0.02	59545.90	16.768
0.2	0.03	59691.53	18.407

0.2	0.04	59945.85	19.663
0.2	0.05	60328.80	20.878
0.2	0.06	60791.40	21.950
0.2	0.07	61178.70	22.883
0.2	0.08	61653.44	23.805
0.2	0.09	62124.28	24.670
0.2	0.10	62706.70	25.515
0.4	0.00	92039.20	8.527
0.4	0.01	90544.87	25.760
0.4	0.02	90125.34	29.972
0.4	0.03	89995.23	32.738
0.4	0.04	90052.32	34.833
0.4	0.05	90377.86	36.819
0.4	0.06	90786.71	38.545
0.4	0.07	91255.45	40.141
0.4	0.08	91574.83	41.475
0.4	0.09	92074.75	42.856
0.4	0.10	92498.82	44.050
0.6	0.00	157329.34	17.829
0.6	0.01	153317.54	54.931
0.6	0.02	152039.83	63.338
0.6	0.03	151710.69	69.033
0.6	0.04	151525.90	73.349
0.6	0.05	151572.74	77.028
0.6	0.06	151296.54	80.190
0.6	0.07	151758.66	83.058
0.6	0.08	152377.72	85.796
0.6	0.09	152972.00	88.617
0.6	0.10	153712.48	91.191
0.8	0.00	354791.47	57.282
0.8	0.01	342299.05	178.538
0.8	0.02	338196.35	204.670
0.8	0.03	337241.18	223.619
0.8	0.04	335601.10	235.917

0.8	0.05	334513.48	247.288
0.8	0.06	333676.63	256.211
0.8	0.07	333880.38	264.568
0.8	0.08	336235.61	276.138
0.8	0.09	336194.78	281.543
0.8	0.10	337909.40	290.923

Table 3: Numerical estimate of the residence time in the cases discussed in Section 6.4. Recall $L_2 = 200$ and $\delta = 0$.

References

[1] D. Andreucci, D. Bellaveglia, E.N.M. Cirillo, "A model for enhanced and selective transport through biological membranes with alternating pores." *Mathematical Biosciences* **257**, 42–49 (2014).

[2] D. Andreucci, D. Bellaveglia, E.N.M. Cirillo, S. Marconi, "Effect of intracellular diffusion on current–voltage curves in potassium channels." *Discrete and Continuous Dynamical System Series B* **19**, 1837–1853 (2014).

[3] D. Andreucci, D. Bellaveglia, E.N.M. Cirillo, S. Marconi, "Monte Carlo study of gating and selection in potassium channels." *Physical Review E* **84**, 021920 (2011).

[4] V.I. Arnold, "Ordinary Differential Equations." Third edition, Springer–Verlag, Berlin Heidelberg, 1992.

[5] J. Barrera, O. Bertoncini, R. Fernández, "Abrupt convergence and escape behavior for birth and death chains." *J. Stat. Phys.* **137**, 595–623 (2009).

[6] C. Bahadoran, T.S. Mountford, "Convergence and local equilibrium for the one–dimensional nonzero mean exclusion process." *Probability Theory and Related Fields* **136**, 341–362 (2006).

[7] L. Bertini, A. De Sole, D. Gabrielli, G. Jona–Lasinio, C. Landim, "Large deviations for the boundary driven simple exclusion process." *Math. Phys. Anal. Geom.* **6**, 231–267 (2003).

[8] R.A. Blythe, M.R. Evans, "Nonequilibrium steady states of matrix product form: a solver's guide." Preprint arXiv:0706.1678.

[9] E.N.M. Cirillo, A. Muntean, "Can cooperation slow down emergency evacuations?" *Comptes Rendus Macanique* **340**, 6260-628 (2012).

[10] E.N.M. Cirillo, A. Muntean, "Dynamics of pedestrians in regions with no visibility – a lattice model without exclusion." *Physica A* **392**, 3578–3588 (2013).

[11] B. Derrida, M.R. Evans, V. Hakim, V. Pasquier, "Exact solution of a $1D$ asymmetric exclusion model using a matrix formulation." *Journal of Physics A: Mathematics and General* **26**, 1493–1517 (1993).

[12] B. Derrida, S.A. Janowsky, J.L. Lebowitz, E.R. Speer, "Exact solution of the totally asymmetric simple exclusion process: shock profiles." *J. Stat. Phys.* **73**, 813–842 (1993).

[13] A. De Masi, P. Ferrari, "Flux fluctuations in the one dimensional nearest neighbors symmetric simple exclusion process." *J. Stat. Phys.* **107**, 677–683 (2002).

[14] D. Desirable, P. Dupont, M. Hellou, S. Kamali–Bernard, "Cellular automata in complex matter." *Complex Systems* **20**, 67–91 (2011).

[15] P.A. Fedders, "Two–point correlation functions for a distinguishable particle hopping on a uniform one-dimensional chain." *Physical Review B* **17**, 40 (1978).

[16] F.J.M.M. de Gauw, J. van Grondelle, R.A. van Santen, "Effects of single–file diffusion on the kinetics of hydroisomerization catalyzed by Pt/H–Mordenite." *Journal of Catalysis* **204**, 53–63 (2001).

[17] M. Gorissen, A. Lazarescu, K. Mallick, C. Vanderzande, "Exact current statistics of the asymmetric simple exclusion process with open boundaries." *Phys. Rev. Lett.* **109**, 170601 (2012).

[18] K. Hahn, J. Kärger, "Deviations from the normal time regime of single–file diffusion." *Journal of chemical physics B* **102**, 5766–5771 (1998).

[19] K. Kosmidis, P. Argyrakis, P. Macheras, "A reappraisal of drug release laws using Monte Carlo simulations: the prevalence of the Weibull function." *Pharmaceutic Research* **20**, (7), 988–995 (2003).

[20] A. Muntean, E.N.M. Cirillo, O. Krehel, M. Bohm, "Pedestrians moving in dark: Balancing measures and playing games on lattice." In "Collective Dynamics from Bacteria to Crowds", An Excursion Through Modeling, Analysis and Simulation Series: CISM International Centre for Mechanical Sciences, Vol. 553 Muntean, Adrian, Toschi, Federico (Eds.) 2014, VII, 177 p. 29 illus, Springer, 2014.

[21] F. Rezakhanlou, "Hydrodynamic limit for attractive particle systems on $\mathbb{Z}^d$." *Comm. Math. Phys.* **140**, 417–448 (1991).

[22] M.J. Simpson, K.A. Landman, B.D. Hughes, "Multi–species simple exclusion processs." *Physica A* **388**, 399–406 (2009).

[23] M.R. Evans, N. Rajewsky, E.R. Speer, "Exact solution of a cellular automaton for traffic." *Journal of Statistical Physics* **95**, 45–96 (1999).

PREVIOUS PUBLICATIONS IN THIS SERIES:

Number	Author(s)	Title	Month
14-29	C.R. Prins J.H.M. ten Thije Boonkkamp W.L. IJzerman T.W. Tukker	A least-squares method for optimal transport using the monge-ampère equation	Sept. '14
14-30	N. Kumar J.H.M. ten Thije Boonkkamp B. Koren	A sub-cell discretization method for the convective terms in the incompressible Navier-Stokes equations	Oct. '14
14-31	M. Redeker I.S. Pop C. Rohde	Upscaling of a tri-phase phase-field model for precipitation in porous media	Oct. '14
14-32	P.J.P. van Meurs A. Muntean	Upscaling of the dynamics of dislocation walls	Nov. '14
14-33	E.N.M. Cirillo A. Muntean R.A. van Santen A. Sengar	Residence time estimates for asymmetric simple exclusion dynamics on stripes	Nov. '14